Biosensors and Bioelectronics 25 (2009) 702–707

Contents lists available at ScienceDirect

Biosensors and Bioelectronics

journal homepage: www.elsevier.com/locate/bios

Triple-helix DNA structural studies using a Love wave acoustic biosensor

George Papadakis[a,b], Achilleas Tsortos[a], Electra Gizeli[a,b,*]

[a] Institute of Molecular Biology and Biotechnology, FO.R.T.H, Vassilika Vouton, 71110, Heraklion, Greece
[b] Department of Biology, University of Crete, Vassilika Vouton, 71409, Heraklion, Greece

ARTICLE INFO

Article history:
Received 16 June 2009
Received in revised form 6 August 2009
Accepted 7 August 2009
Available online 15 August 2009

Keywords:
TFO
Love wave sensor
Triplex DNA
DNA intrinsic viscosity

ABSTRACT

The development of sensors for detecting the conformation of surface-attached molecules is an emerging field with significance in the pharmaceutical industry and in drug design. In this work, triplex-forming oligos (TFOs), a separate class of non-natural DNA bending agents that can affect the mechanical properties of DNA through the formation of triple-helical structures of specific conformation and/or flexibility, are used as a model system in combination with an acoustic biosensor to determine molecular geometrical features. In practice, the degree of bending of a specific DNA target caused by a particular TFO was evaluated by measuring the ratio of acoustic energy change over phase change observed during the binding of pre-formed triplex DNA molecules to the device surface. The DNA bending angle derived via acoustic measurements is in excellent agreement with previously reported values using molecular biology techniques. The reported acoustic technique appears quite appealing for the biophysical study of DNA molecules providing rapid qualitative and quantitative information, at the same time holding promise to be developed as a high-throughput method for the evaluation of DNA conformational changes.

1. Introduction

Analysis of a specific DNA sequence is an increasingly important area in bioanalytical sciences as the genetic basis of many diseases is elucidated. For this reason, considerable effort is directed towards the development of techniques and devices for studying DNA with emphasis in detecting single mismatches via a hybridization process. Such devices are based on either the detection of the presence of a specific label, such as a fluorophore, or on label-free detection using optical or acoustic biosensors (Cosnier and Mailley, 2008; Vercoutere and Akeson, 2002). Regardless of the presence or absence of label molecules, all the above methodologies provide signals which can be related to the mass of the bound DNA molecule.

In addition to the detection of DNA mismatches in hybridization assays, DNA conformation is another parameter of interest affecting various biological functions within the cell. It is now recognized that specific geometrical features of DNA molecules such as intrinsic DNA bending as well as conformational changes induced by ligand binding, play an important role in transcription, replication, DNA packing and repair (Dlakic and Kerppola, 2001). Consequently, by controlling the structural features of DNA, these processes and especially gene expression can be regulated to correct for cell malfunctions and to prevent the development of severe genetic diseases and cancer (Bednarski and Firestine, 2006; Nayak et al., 2006). Furthermore, structural DNA nanotechnology is an emerging field which deals with building DNA molecules with particular geometrical features; changing DNA shape in a controlled way, i.e. in response to an external stimulus, allows the creation of a nanomachinery (Seeman, 2005). Such molecular switches include molecular beacons which are single-stranded oligonucleotide hybridization probes that form a stem-and-loop structure (Drake and Tan, 2004) or two-stage molecular recognition DNAs that undergo conformational change upon hybridization and exposure to Mg^{2+} (Buck et al., 2007).

Despite the biological and bioanalytical importance in detecting DNA conformation, the development of such devices is currently limited. Of the available systems, acoustic devices appear to be good candidates for providing structural information of surface-attached molecules (Wang et al., 2006; Carmon et al., 2005), based on the wave's sensitivity to other parameters than just mass. Generally, several mathematical models have appeared trying to explain experimental results (Voinova et al., 1999; MacMullen et al., 2000; Johannsmann, 2008). The most common approaches are based on the fact that acoustic energy can sense the viscosity or viscoelasticity of a liquid solution or film, respectively, attached to the device surface. When the sensing sample is modeled as a film, then energy measurements can be related to the viscoelasticity of the layer which is determined by the amount of trapped water within the film and the nature and conformation of the adsorbed molecules

* Corresponding author at: Institute of Molecular Biology and Biotechnology, FO.R.T.H, Vassilika Vouton, 71110, Heraklion, Greece. Tel.: +30 2810 394373; fax: +30 2810 394408.
E-mail address: gizeli@imbb.forth.gr (E. Gizeli).

0956-5663/$ – see front matter © 2009 Elsevier B.V. All rights reserved.
doi:10.1016/j.bios.2009.08.015

(Su et al., 2005). In this case, the physical model used for the quantitative interpretation of experimental data can give information on the shear viscosity and modulus of the film, which, in turn, can be related to its morphology. The above analysis was used to investigate the viscoelastic properties of single and double-stranded templates during DNA hybridization (Stengel et al., 2005).

An alternative approach presented recently, is based on correlating acoustic energy to the viscosity of a sample solution present at the device/liquid interface. Binding of discrete DNA molecules alters the viscosity of the interface in a manner that is related to the molecules' intrinsic viscosity. The latter was shown to be related to the geometrical characteristics and internal structure of the attached molecules. As a result, acoustic measurements, in combination with a suitable mathematical treatment, were used to provide quantitative information on the conformation of surface-tethered DNA molecules, distinguishing between DNAs of different length, bending angle and shape (Tsortos et al., 2008a,b,c).

The purpose of the present work was to further verify the above approach and show the general applicability of the acoustic technique. Artificial DNA ligands, such as triplex-forming oligonucleotides, designed to bind and induce a specific bend during triple-helix formation were used. Triple-helix formation is the result of sequence specific binding of oligonucleotides to the major groove of double-stranded DNA through the formation of Hoogsteen hydrogen bonds with purine bases (Faria and Giovannangeli, 2001; Seidman and Glazer, 2003; Fox, 2000; Vasquez and Glazer, 2002). Apart from their ability to induce DNA bending, TFOs were also chosen for their extensive biomedical and pharmacological applications described in various reviews (Escude and Sun, 2005; Maiti and Kumar, 2007; Vasquez and Glazer, 2002). Currently, TFO binding affinities and binding specificity to a duplex DNA can be estimated by fluorescent methods (Darby et al., 2002; Reither and Jeltsch, 2002) and gel assays (Kalish et al., 2005; Olivas and Maher, 1996); both techniques have also been used to provide structural insights on DNA bending induced by TFOs (Akiyama and Hogan, 1996, 1997; Liberles and Dervan, 1996). However, the above methods are semi-quantitative and not applicable to rapid analysis and high-throughput screening.

In the current work, two sets of TFOs were employed, designed to bind either without affecting the structure (TFO10) or by inducing a bend (TFO4), both resulting in triple-helix formation (Liberles and Dervan, 1996). Furthermore, the specific DNA bending angle, quantified in a previous study using phasing analysis (Liberles and Dervan, 1996) was used to evaluate our approach.

2. Materials and methods

2.1. Acoustic wave device and instrumentation

Surface acoustic wave (SAW) devices supporting shear horizontal waves were prepared by photolithography using single-crystal Y-cut z-propagating 0.5 mm thick quartz, with a 100 nm gold overlayer on top of a 20 nm chromium adhesion layer (Fig. 1). The input and output interdigitated transducers (IDTs) consisted of 192 pairs of split fingers with a periodicity of 32 μm. The operating frequency of the SAW device was 155 MHz. A 0.4 μm thick waveguide layer of poly(methyl methacrylate) (PMMA) was deposited on the surface of the acoustic device by spin-coating at 4000 rpm

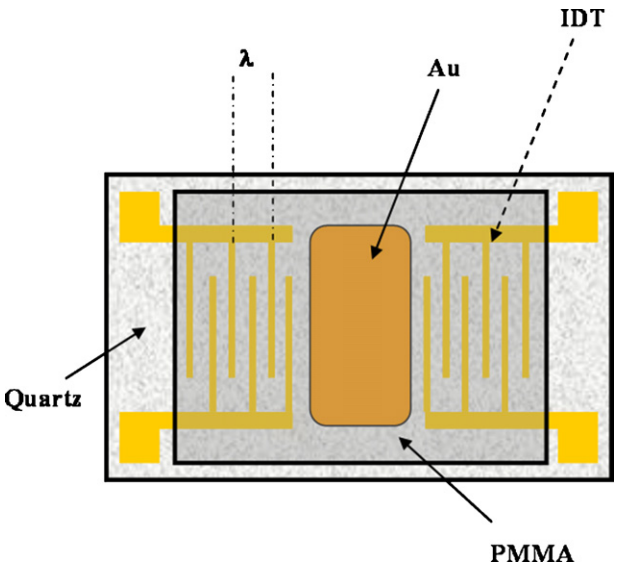

Fig. 1. Schematic representation of the acoustic device: top-view, showing the quartz piezoelectric crystal, the imprinted IDTs (the wave length of the acoustic signal is $\lambda \approx 32\,\mu m$) and the PMMA and gold layers.

with a 8% (w/w) solution of medium molecular weight PMMA in 2-ethoxyethylacetate (Aldrich). PMMA is used to enhance the signal however, its absolute thickness is not involved in the analysis carried out. The PMMA-covered devices were heated to 195 °C for 2 h to promote solvent evaporation. Devices were re-used by cleaning off adsorbed samples with a swab stick soaked in ethanol. An Agilent E5061A network analyzer was used to measure the energy (amplitude) and phase of the output signal with respect to a reference one. Data was collected using LabVIEW interface software. A perspex flow cell and a silicone rubber gasket were used to hold the solution in place over the region between the IDTs, exposing an area of 12 mm^2.

2.2. Target DNA design and preparation

Two different double-stranded DNA molecules (50 and 100 bp in length) were designed to contain two distal binding sites located at the centre of the sequence separated by one turn of the DNA helix. Each site consisted of 15 bp purine tracts and could be targeted simultaneously by a TFO containing two 15-base pyrimidine tracts (Fig. 2).

The construction of the 100 bp DNA molecules required the design and purchase of an oligonucleotide 70-bases long (oligo70: 5′-acggccagtgaattcagagaggaggagagagcggtgc ggtaggagagagagaggaggatcctcgagagtc-3′) from Metabion (Germany), which contained the two distal sites flanged by two restriction sites recognized by the EcoRI and BamHI endonucleses, respectively. The oligo70 was rendered double-stranded and amplified in a standard PCR reaction using the appropriate forward (p1: 5′-acggccagtgaattcagag-3′) and reverse (p2: 5′-gactctcgaggatcctcct-3′) primers, purchased from Metabion. The PCR product was gel-extracted and purified using Nucleospin extraction kit (Macherey-Nagel) then digested with EcoRI and

Site 1 Site 2
(100) cacaggaaacagctatgacatgattacgaattc agagaggagaagaga gcggtgcggt aggagagagagagga ggatcctctagagtcgacctggaggca

Site 1 Site 2
(50) aattc agagaggagaagaga gcggtgcggt aggagagagagagga ggatc

Fig. 2. Base sequence of the two DNA strands.

BamHI restriction enzymes purchased from Minotech (Greece) and finally cloned into Puc18 vector purchased from Minotech. Plasmid isolation and purification were accomplished following the manufacturer's instructions of the Plasmid Purification Kit (Genomed). The recombinant plasmid was verified by diagnostic digestions and a sequencing reaction performed at the sequencing facility centre at IMBB (Heraklion). Sequencing results were used to design one set of primers in order to produce the 100 bp product. The set of primers included one 5′-end-biotinylated forward primer (5′-biotin-cacaggaaacagctatgac-3′) and a non-biotinylated reverse one (5′-tgcctgcaggtcgactc-3′) resulting in the production of one-end-bioinylated PCR products. A Nucleospin column was again used for the purification of the PCR products. The 50 bp long double-stranded DNA was prepared by annealing a 5′-biotinylated oligo with its complementary strand. A 50 μl mixture of the two oligos (annealing buffer contained 1 mM $MgCl_2$ and 50 mM Tris pH 7.5) was vortexed, heated-up at 95 °C for 5 min and then cooled slowly at room temperature for approximately 10 min. HPLC purified oligos were purchased from Metabion with the following sequences:

First strand: 5′-biotin-aattcagagaggaggagagagcggtgcggtaggagaga-gagaggaggatc-3′
Second strand: 5′-gatcctcctctctctctcctaccgcaccgctctctcctcctctctg-aatt-3′

2.3. TFO design

Two different TFOs were designed in order to be capable of forming a triple-helix with each of the two DNA targets. The first one (TFO4: 5′-*t*c*t*c*t*c*c*t*c*c*t*c*t*c*t*ttttttc*c*t*c*t*c*t*c*t*c*c*t-3′, *c* is 5-methyl cytosine) contained two 15-base pyrimidine tracts separated by a 4-nucleotide linker. TFO4 could simultaneously form a triple-helix with the DNA targets and force them to bend, with a bend angle that was previously estimated to be 119 ± 3° (Liberles and Dervan, 1996). A second triplex-forming oligo (TFO10: 5′-*t*c*t*c*t*c*c*t*c*c*t*c*t*c*t*ttttttttttttc*c*t*c*t*c*t*c*t*c*c*t-3′, *c* is 5-methyl cytosine) contained also the two pyrimidine tracts and a 10-nucleotide linker which could fit in the DNA helix turn separating the two distal binding sites. TFO10 could form a triple-helix with the DNA targets without bending them significantly. Both TFOs were modified with 5-methyl cytosines since they form an extra spine of methyl groups that increase the stability of the triple-helix (Fox, 2000). Modified TFOs were purchased and HPLC purified from Metabion (Germany). Fig. 3 depicts the full set of 100 and 50 base pair duplex and triplex DNAs used in this work.

2.4. Triple-helix formation

Triple-helix formation was performed by incubating 200 picomoles of the modified oligo with approximately 100 ng/μl from each of the three DNA targets at 22 °C for at least 1 h. Reaction volume was between 10 and 20 μl and the incubation buffer contained 45 mM Mes (2-[N-morpholino] ethanesulphonic acid), pH 5.5 with 1 mM $MgCl_2$. Successful triple-helix formation was verified by running a 12% polyacrylamide gel at 4 °C (60 V, 4 h) in the same buffer. The gel was adequately stained for 30 min with ethidium bromide (Akiyama and Hogan, 1996; Mergny et al., 1991) and visualized under a UV lamb. Triple DNA molecules were observed to migrate slower compared to the respective duplexes (Liberles and Dervan, 1996) (Fig. 4).

2.5. Real-time acoustic measurements

For the immobilization of the triple stranded DNA on the surface the neutravidin–biotin approach was used. A continuous flow of buffer (45 mM Mes pH 7.5 and 1 mM $MgCl_2$) was pumped over the surface of the devices at a flow rate of 20 μl/min (shear rate 1.9 s^{-1}). The signal was allowed to equilibrate prior to the first addition and all samples were added in the same buffer. Neutravidin (Pierce, specific activity 11–17 μg biotin bound/mg protein) was added at a concentration of 100 μg/ml for 10 min, long enough to saturate the surface with a large excess of protein. After a buffer rinse, pre-incubated 1–2 μg/ml of biotinylated DNA triplexes were added and acoustic data were collected every 2 s.

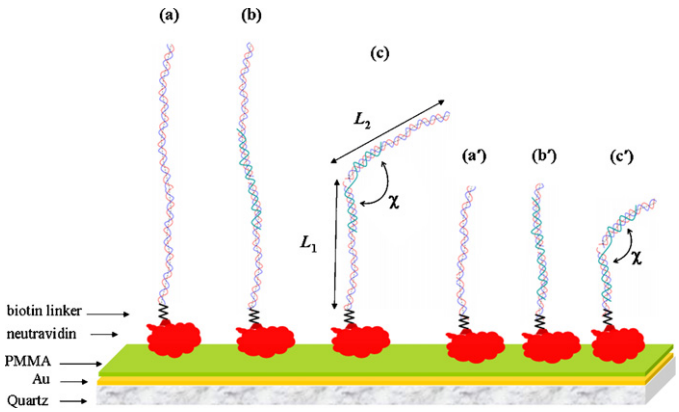

Fig. 3. Schematic representation of the biosensor device surface. DNA molecules were attached to the neutravidin-modified PMMA surface through a biotin linker incorporating an 11-carbon hinge. DNA molecules include: (a) double-stranded DNA 100 bp long; (b) triple stranded "straight" DNA 100 bp long formed upon incubation of (a) with TFO10; (c) triple stranded "bent" DNA 100 bp long formed upon incubation of (a) with TFO4; (a′), (b′) and (c′): as above with 50 bp DNAs. All DNAs were drawn using the GSVIEW software package (http://www.lfd.uci.edu/~gohlke/curve/).

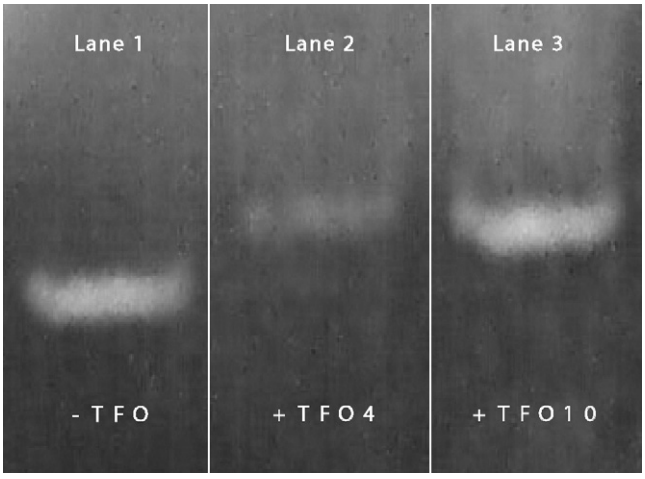

Fig. 4. Successful triple-helix formation verified by a 12% polyacrylamide gel stained with ethidium bromide. Lane 1 corresponds to a 100 bp duplex DNA, while lanes 2 and 3 correspond to the triplexes formed by the addition of the TFO4 and TFO10, respectively. Triple DNA molecules can be observed to migrate slower compared to the respective duplex.

2.6. Acoustic wave sensor and modeling

The work described here was carried out with a Love wave device (Fig. 1); extensive information on the Love wave device can be found elsewhere (Gizeli, 2000; Ballantine et al., 1997). Application of a viscous liquid to the device surface would result primarily in energy dissipation, measured as amplitude change (Ballantine et al., 1997; Saha et al., 2003; Mitsakakis et al., 2008). The penetration depth δ of the wave inside the liquid sample, i.e. the distance

from the device surface within which acoustic sensing takes place, is given as $\delta = (2\eta/\omega\rho)^{1/2}$, where η and ρ are the solution viscosity and density, respectively, and ω is the oscillation angular frequency. At the 155 MHz operating frequency of the Love wave device, δ is 45 nm for pure water, well above the length of the longest DNA tested here.

The attachment of molecules on the device surface in the presence of a liquid sample (e.g. buffer) can be treated as neither a purely elastic, nor a viscous liquid layer. Recently, DNA molecules anchored to the device surface were modeled as discrete molecules affecting the viscosity of the sample at the device/liquid interface. In this work, changes in the measured ratio of amplitude change over phase change ($\Delta A/\Delta Ph$), i.e. energy dissipation per coupled unit mass, recorded during DNA binding, parallel changes in the intrinsic viscosity [η] of bound molecules (Tsortos et al., 2008a,b,c).

Double-stranded DNA molecules with a "bent" rod conformation and of various bend angles can be modeled as having two rod-like arms of lengths L_1 and L_2 joined end-to-end at an angle χ (Fig. 3). The two components have the same diameter D and the total length is L, where $L = L_1 + L_2$. Their hydrodynamic behavior has been extensively studied theoretically using a "bead" model. Calculations based on this model take the macromolecule as being composed of spherical elements (beads) and correlate the ratio of intrinsic viscosities $[\eta]_{\text{"bent"}}/[\eta]_{\text{"straight"}}$ to the specific bending angle of the "bent" rod for any particular ratio of L_1 to L_2 (Garcia de la Torre and Bloomfield, 1978, 1981). Since the acoustic ratio is also a measure of the molecule's intrinsic viscosity, the above implies that the ratio of $(\Delta A/\Delta Ph)_{\text{"bent"}}/(\Delta A/\Delta Ph)_{\text{"straight"}}$ can be also used to calculate the angle of the "bent" molecule. A detail description of this approach can be found in the following publications (Tsortos et al., 2008a,b).

3. Results

3.1. Acoustic measurements

Biotinylated triplex DNA molecules of 50 and 100 bp were preformed during incubation of the DNA target molecules with the two triplex-forming oligos for 1 h at room temperature. Polyacrylamide gel images verified the successful and complete (100%) triplex formation of all DNA targets. Pre-formed triplexes were bound to a neutravidin-modified device surface by using biotin attached to the 5′-end of the DNA molecule through a hinge of eleven carbon atoms. Experiments were performed in a flow-through system which allowed continuous additions of DNA samples and buffer in an alternating way. DNA binding resulted in a change of both amplitude and phase, as these were simultaneously recorded in real-time with the network analyzer (Fig. 5). Acoustic results were expressed as the ratio of amplitude change over phase change ($\Delta A/\Delta Ph$) (Table 1). This ratio was previously demonstrated to be independent of the DNA sample loading concentration and, thus, DNA surface coverage (Tsortos et al., 2008a,b,c).

A critical issue related to the acoustic measurements was the pH of the running buffer. Triplex formation and stability require a low pH buffer (less than 6) which is the reason why Mes pH 5.5 was also selected as the running buffer for the acoustic measurements. However, at that pH the preadsorbed neutravidin layer (pI = 6.3) becomes positively charged and non-specific interactions with the negatively charged DNA can not be avoided. Although, control experiments with non-biotinylated oligonucleotides revealed their ability to bind to neutravidin, this particular non-specific interaction was also shown to be reversible since oligonucleotides could be washed away with buffer rinsing (data not shown). Furthermore, the acoustic ratios were measured during the binding of double-stranded biotinylated DNA molecules 50 and 100 bp long to the neutravidin-modified surface for two different running buffers; one at pH 5.5 (Mes/$MgCl_2$) and another at pH 7.2 (Tris/$MgCl_2$) which is known to prevent non-specific interactions. The acoustic ratios for the 100 bp dsDNA molecules were found to be identical in the two pH buffers: in pH 5.5 was 11.6 ± 1.3 while in pH 7.2 was 11.7 ± 0.3. Additionally, the acoustic ratios for the 50 bp DNA molecules in the two buffers varied by only 10%, which is within the experimental error of acoustic measurements: in pH 5.5 was 8.5 ± 0.6 and in pH 7.2 was 7.6 ± 0.5. Numbers are averages of 2 to 7 repeats. These results clearly show that non-specific interactions due to low pH do not significantly affect the acoustic measurements resulting from the specific immobilization through the extremely strong avidin–biotin bond. Therefore, it was possible to use the low pH running buffer to investigate conformational differences among triplex DNA molecules.

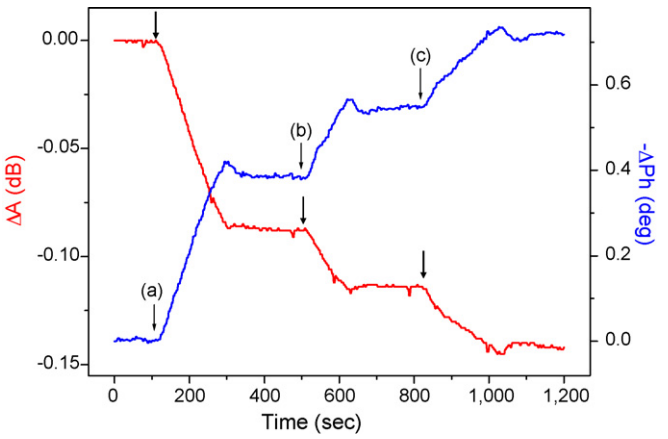

Fig. 5. Real-time data of simultaneously recorded amplitude (ΔA) and phase changes (ΔPh) during the application of: (a) neutravidin 100 μg/ml, followed by two sequential additions of 2 μg/ml of pre-incubated biotinylated 100 bp triplex DNA (b) and (c). Buffer washing steps following each deposition are not shown in the graph.

3.2. Acoustic ratios of "straight" and "bent" duplex and triplex DNAs

Initially, a straight 100 bp DNA triplex was formed after 1 h incubation of the corresponding DNA duplex with the TFO10. The triplex molecule had a rather "straight" conformation, since the 10-base linker of the TFO was designed to fit the central turn of the DNA helix between the two polypurine distal sites. The acoustic ratio ($\Delta A/\Delta Ph$), measured during the binding of the above molecule,

Table 1
Acoustic ratios R observed during the binding of 50 and 100 bp long "straight" double-stranded (ds) and triple stranded (ts) as well as "bent" triple stranded DNA molecules on the device surface. Note that $R = \Delta A/\Delta Ph$, where A and Ph are the acoustic amplitude and phase signals, respectively.

	50		100	
	$\Delta A/\Delta Ph$ (10^{-2} dB/deg)	$R_{\text{"bent"}}/R_{\text{"straight"}}$	$\Delta A/\Delta Ph$ (10^{-2} dB/deg)	$R_{\text{"bent"}}/R_{\text{"straight"}}$
ds "straight"	8.5 ± 0.6		11.6 ± 1.3	
ts "straight"	14.5 ± 0.7	0.86	16.7 ± 0.9	0.88
ts "bent"	12.5 ± 0.6		14.8 ± 0.7	

was found to be 16.7 ± 0.9 (10^{-2} dB/deg) (6 repetitions). In addition, a "bent" triplex with a bend located in the centre of the molecule was also formed after incubation of the 100 bp duplex DNA with the TFO4. This triplex DNA has the same length and molecular weight as the straight 100 bp molecule but adopts a different shape as a result of the specific sequence of the TFO4 ligand. Acoustic measurements obtained during the binding of the 100 bp triplex "bent" molecule provided a ratio of 14.8 ± 0.7 (10^{-2} dB/deg) (6 repetitions). For comparison, the acoustic ratio of the 100 bp DNA duplex was also measured and found to be 11.6 ± 1.3 (10^{-2} dB/deg) (7 repetitions).

The above experiments were also repeated with the 50 bp "straight" duplex and triplex and the 50 bp "bent" triplex DNA molecules; all data are summarized in Table 1.

3.3. Calculation of DNA bend angle

In order to calculate the bend angle of the 100 and 50 bp "bent" triplexes, formed under the effect of the TFO4, the mean acoustic ratio measured for the "bent" triple DNAs was compared to the respective ratio obtained during the binding of the "straight" triplexes, formed with TFO10. The values of the relation $(\Delta A/\Delta Ph)_{\text{"bent"}}/(\Delta A/\Delta Ph)_{\text{"straight"}}$ were found to be 0.88 for the 100 and 0.86 for the 50 bp DNAs. By using the "bead" model (with $L_1 = L_2$ since the bent is induced/located at half length for both the 50 and 100 bp chains) it was possible to produce values for the ratio $[\eta]_{\text{"bent"}}/[\eta]_{\text{"straight"}}$ which is equivalent to the acoustic ratio $(\Delta A/\Delta Ph)_{\text{"bent"}}/(\Delta A/\Delta Ph)_{\text{"straight"}}$ and depends on the bending angle. The calculated with the "bead" model bending angle for both the 100 and 50 bp triplexes was found to be equal to $124 \pm 6^{\circ}$.

4. Discussion

Triplex-forming oligos display the exciting ability to bind sequence-specific double helical DNA in order to form triple-helical structures. Viscosity measurements have long been a standard method for distinguishing structural features/differences in DNA research; observing changes in length and/or shape (long chains or supercoiled molecules, etc.) is a typical example (Suh and Chaires, 1995). Regarding duplex and triplex DNA, comparison between molecules based on their viscosity properties has also been made (Pilch et al., 1993; Scaria and Shafer, 1991).

In this study, acoustic measurements were carried out during the binding of two sets of 50 and 100 bp molecules, each set including a "straight" duplex, a "straight" triplex and a centrally "bent" triplex DNA (Fig. 3). Triplex DNAs with a "bent" or "straight" configuration were formed upon binding of TFOs consisting of two distal DNA sites separated by a 4- or a 10-nucleotide linker, respectively, to double helical DNA targets. Results revealed that all DNA structures could be discriminated on the basis of their acoustic ratio (a measure of the intrinsic viscosity of bound DNAs) reflecting differences in their conformations and internal structure (Table 1); this behavior is consistent with previous studies (Tsortos et al., 2008a,b,c). From a quantitative point of view, acoustic measurements combined with the "bead" model were used to characterize the triple-helical DNAs. Based on the experimental design of TFO4, ligand binding should induce a specific bending angle of the target DNA which would be sequence-specific and independent of DNA length. For the two DNA molecules, this should be reflected in the ratio of $(\Delta A/\Delta Ph)_{\text{"bent"}}/(\Delta A/\Delta Ph)_{\text{"straight"}}$, which is only related to the bend angle. Indeed, the almost identical numbers of 0.88 and 0.86 calculated for the 100 and 50 bp molecules proved the validity of our approach. Furthermore, the employed DNA targets and the particular triplex-forming agent (TFO4) were selected based on a previous study that quantified the bending angle; triplex DNA formed via TFO4 binding was, therefore, used in this work as an external reference to the quantification resulting from acoustic experiments. TFO4-binding to DNA was measured with the sensitive method of phasing analysis to induce a bend angle of $119 \pm 3^{\circ}$ (Liberles and Dervan, 1996), in excellent agreement with the acoustic estimation of $124 \pm 6^{\circ}$.

Besides the quantitative nature of these experiments, the acoustic ratios of the DNA pairs can provide further insight on the internal structure and relative flexibility of the molecules. Of particular interest is our finding that triplex DNAs exhibit higher acoustic ratios (i.e., higher intrinsic viscosities according to our model) than the corresponding duplexes. In lieu of direct experimental data on triplex DNA intrinsic viscosities we seek a qualitative explanation.

Differences in intrinsic viscosity reflect differences on either structural (dimensional) and/or hydration features. Regarding dimensional/structural changes upon formation of the triplex DNA the following is known. It is well established that duplex DNA has a B-like structure (Bloomfield et al., 2000). For triplex DNA, initial X-ray results at low resolution (Arnott and Selsing, 1974) indicated an A-type of structure in contrast to more recent AFM (Hansma et al., 1996) and crystallographic/modeling data (Liu et al., 1996) that suggest more of a B-like structure; A-type is a little shorter-wider helix compared to B-type. Molecular dynamics simulations showed that strand II is in A- while strands I and III are neither in A- nor in B-form (Weerasinghe et al., 1995; Mohan et al., 1993). Lacking a consensus on the structure of the triplex DNA we can only say that even if small differences do exist in either length or width of the double and triple-helical DNAs (with the same number of bases) they are not capable of explaining the big difference in the observed acoustic ratios (Tsortos et al., 2008a,b,c).

On the other hand, it would be expected that the hydration of the triplex and doublex DNA molecules is quite different since both the amount of negative charge (contributed by each base) and its spatial distribution along the axis of the two cylinders is rather different. These differences have been well documented. NMR studies have revealed, along with structural differences, that the amino group of adenine, crucial for the stability of a triple-helix, has a different hydration pattern than that in the doublex (Radhakrishnan and Patel, 1994; Jiang and Russu, 2002).

Molecular dynamics simulations (Weerasinghe et al., 1995; Mohan et al., 1993) comparing doublex and triplex DNA concluded that there is a difference in the spine hydration between strands I and III and also suggest that triplex DNA is more rigid than duplex.

It may be argued then that formation of a triple-helix is, primarily, a phenomenon that results in alteration of the molecular weight, density and charge of a double helical DNA without affecting its diameter or length significantly (Vasquez and Glazer, 2002). The introduction of the polyanionic third strand, does not affect the size of the duplex molecule so much as its internal structure, charge and, consequently, hydration (Weerasinghe et al., 1995). The different water arrangement, mobility and ion condensation atmospheres around the two molecules (Shields et al., 1997; Berman, 1991) could lead to different intrinsic viscosities.

The above changes that occur upon triplex formation were clearly observed in this work as a difference in the acoustic ratios measured for the triplex 100 and 50 bp molecules compared to the respective duplexes.

5. Conclusions

The geometrical characteristics of DNA molecules resulting from the formation of triple-helical DNAs have been evaluated using an acoustic Love wave device. Acoustic data were used to quantify the degree of bending of a triple-helical DNA molecule and detect mechanical changes between double and triple-helical molecules.

This work opens up the possibility to employ acoustic biosensors for the biophysical study of DNA molecules and their mechanical properties. Furthermore, the sensitive and quantitative nature of the method offers the advantage of the rapid and simple evaluation of all the factors related to triplex formation including sequence specificity and stability, degree of bending and flexibility of the DNA molecule. The above are extremely important in the evaluation of TFO agents (drugs) designed with the potential to target specific regions on DNA for therapeutic purposes. The acoustic technique combines the potential to be developed as a drug screening method for high-throughput qualitative and quantitative measurements of DNA conformational changes.

Acknowledgement

The authors would like to acknowledge the Human Frontier Science Program (HFSP) for financially supporting this work.

References

Akiyama, T., Hogan, M.E., 1996. Proc. Natl. Acad. Sci. U.S.A. 93, 12122–12127.
Akiyama, T., Hogan, M.E., 1997. Biochemistry 36, 2307–2315.
Arnott, S., Selsing, E., 1974. J. Mol. Biol. 88, 509–521.
Ballantine, D.S., White, R.M., Martin, S.J., Ricco, A.J., Zellers, E.T., Frye, G.C., Wohltjen, H., 1997. Acoustic Wave Sensors. Academic Press, San Diego, CA.
Bednarski, D., Firestine, S.M., 2006. Chembiochem 7, 1715–1721.
Berman, H.M., 1991. Curr. Opin. Struc. Biol. 1, 423–427.
Bloomfield, V.A., Crothers, D., Tinoco, M.I., 2000. Nucleic Acids. University Science Book, Sausalito, CA.
Buck, A.H., Campbell, C.J., Dickinson, P., Mountford, C.P., Stoquert, H.C., Terry, J.G., Evans, S.A.G., Keane, L.M., Su, T.-J., Mount, A.R., Walton, A.J., Beattie, J.S., Crain, J., Ghazal, P., 2007. Anal. Chem. 79, 4724–4728.
Carmon, K.S., Baltus, R.E., Luck, L.A., 2005. Anal. Biochem. 345, 277–283.
Cosnier, S., Mailley, P., 2008. Analyst 133, 984–991.
Darby, R.A.J., Sollogoub, M., McKeen, C., Brown, L., Risitano, A., Brown, N., Barton, C., Brown, T., Fox, K.R., 2002. Nucleic Acids Res. 30, e39.
Dlakic, M., Kerppola, T.K., 2001. Encyclopedia of Life Sciences. Nature Publishing Group, pp. 1–10.
Drake, T.J., Tan, W., 2004. Appl. Spectrosc. 58, 269A–280A.
Escude, C., Sun, J.S., 2005. Top. Curr. Chem. 253, 109–148.
Faria, M., Giovannangeli, C., 2001. J. Gene Med. 3, 299–310.
Fox, K.R., 2000. Curr. Med. Chem. 7, 17–37.
Garcia de la Torre, J., Bloomfield, V.A., 1978. Biopolymers 17, 1605–1627.
Garcia de la Torre, J., Bloomfield, V.A., 1981. Q. Rev. Biophys. 14, 81–139.
Gizeli, E., 2000. Anal. Chem. 72, 5967–5972.
Hansma, H.G., Revenko, I., Kim, K., Laney, D.E., 1996. Nucleic Acids Res. 24, 713–720.
Jiang, L., Russu, I.M., 2002. Biophys. J. 82, 3181–3185.
Johannsmann, D., 2008. Phys. Chem. Chem. Phys. 10, 4516–4534.
Kalish, J.M., Seidman, M.M., Weeks, D.L., Glazer, P.M., 2005. Nucleic Acids Res. 33, 3492–3502.
Liberles, D.A., Dervan, P.B., 1996. Proc. Natl. Acad. Sci. U.S.A. 93, 9510–9514.
Liu, K., Sasisekharan, V., Miles, H.T., Raghunathan, G., 1996. Biopolymers 39, 573–589.
Maiti, M., Kumar, G.S., 2007. Med. Res. Rev. 27, 649–695.
MacMullen, C., Mehta, H., Gizeli, E., Lowe, C., 2000. J. Phys. D: Appl. Phys. 33, 3053–3059.
Mergny, J.L., Collier, D., Rougee, M., Montenay-Garestier, T., Helene, C., 1991. Nucleic Acids Res. 19, 1521–1526.
Mitsakakis, K., Tserepi, A., Gizeli, E., 2008. J. Microelectromech. Syst. 17, 1010–1019.
Mohan, V., Smith, P.E., Pettitt, B.M., 1993. J. Am. Chem. Soc. 115, 9297–9298.
Nayak, A., Khare, P., Chourasia, M.K., Silakari, O., Kohli, D.V., 2006. Ind. J. Pharm. Sci. 68, 697–704.
Olivas, W.M., Maher III, L.J., 1996. Nucleic Acids Res. 24, 1758–1764.
Pilch, D.S., Waring, M.J., Sun, J.S., Rougee, M., Nguyen, C.H., Bisagni, E., Garestier, T., Helene, C., 1993. J. Mol. Biol. 232, 926–946.
Radhakrishnan, I., Patel, D.J., 1994. Biochemistry 33, 11405–11416.
Reither, S., Jeltsch, A., 2002. BMC Biochem. 3, 27–36.
Saha, K., Bender, F., Rasmusson, A., Gizeli, E., 2003. Langmuir 19, 1304–1311.
Scaria, P.V., Shafer, R.H., 1991. J. Biol. Chem. 266, 5417–5423.
Seeman, N.C., 2005. Trends Biochem. Sci. 30 (3), 119–125.
Seidman, M.M., Glazer, P.M., 2003. J. Clin. Invest. 112, 487–494.
Shields, G.A., Laughton, C.A., Orozco, M., 1997. J. Am. Chem. Soc. 119, 7463–7469.
Stengel, G., Hook, F., Knoll, W., 2005. Anal. Chem. 77, 3709–3714.
Su, X., Wu, Y., Knoll, W., 2005. Biosens. Bioelectron. 21, 719–726.
Suh, D., Chaires, J.B., 1995. Bioorg. Med. Chem. 3, 723–728.
Tsortos, A., Papadakis, G., Mitsakakis, K., Melzak, K.A., Gizeli, E., 2008a. Biophys. J. 94, 2706–2715.
Tsortos, A., Papadakis, G., Gizeli, E., 2008b. Biosens. Bioelectron. 24, 836–841.
Tsortos, A., Papadakis, G., Gizeli, E., 2008c. IEEE International Frequency Control Symposium, FCS, art. no. 4623017, pp. 346–349, doi:10.1109/FREQ.2008.4623017.
Vasquez, K.M., Glazer, P.M., 2002. Q. Rev. Biophys. 35, 89–107.
Vercoutere, W., Akeson, N., 2002. Curr. Opin. Chem. Biol. 6, 816–822.
Voinova, M.V., Rodahl, M., Jonson, M., Kasemo, B., 1999. Phys. Scr. 59, 391–396.
Wang, J.S., Ellis, E.-L., Sundaram, L.P., Thompson, M., 2006. Mol. Biosyst. 2, 184–192.
Weerasinghe, S., Smith, P.E., Mohan, V., Cheng, Y.K., Pettitt, B.M., 1995. J. Am. Chem. Soc. 117, 2147–2158.